

Integrating Distributed Acoustic Sensing for Damage Detection in Old Pre-Stressed Concrete Girders: Preliminary Experimental Results

Lisa Strasser¹, Werner Lienhart¹, Thomas Moser¹, Andrej Anžlin², Mirko Kosič², Maja Kreslin², Doron Hekič²

¹Institute of Engineering Geodesy and Measurement Systems, Faculty of Mathematics, Physics and Geodesy, Graz University of Technology, Steyrergasse 30, 8010 Graz, Austria

²Slovenian National Building and Civil Engineering Institute, Dimičeva ulica 12, 1000 Ljubljana, Slovenia
email: lisa.strasser@tugraz.at

ABSTRACT: In this study, we investigate the load-bearing capacity of pre-stressed concrete girders under various damage levels. We employed Distributed Acoustic Sensing (DAS) technology to monitor and quantify changes in the girder response as damage levels were incrementally introduced. This approach enabled the real-time measurement of dynamic behavior over the entire length of the girder, allowing for a detailed characterization of damage-induced structural changes. To complement the DAS-based approach, we also applied classical acceleration-based damage detection techniques. By integrating these methods, we aimed to cross-validate the results and provide a more comprehensive understanding of damage progression and its impact on structural performance.

The experimental campaign, conducted in Ljubljana, ZAG, involved full-scale testing of pre-stressed concrete girders subjected to controlled damage scenarios. This setup ensured a realistic assessment of the girders' residual capacity and failure mechanisms. The paper presents preliminary results from this experimental study, emphasizing the capability of DAS measurements to detect and characterize damage, while also comparing its performance against traditional methods. By combining advanced sensing technologies with established techniques, this research highlights the potential of DAS as a transformative tool in structural health monitoring.

KEY WORDS: Distributed Acoustic Sensing; Distributed Fiber Optic Sensing; Structural Health Monitoring; Frequency Analysis; Load Test; Infrastructure Monitoring; Bridge Monitoring.

1 INTRODUCTION

Structural Health Monitoring (SHM) of civil structures is gaining more and more significance in the recent years, especially in the case of bridges, since many of them are coming to the end of their design life time or even have to be replaced earlier due to increased loads on the structure. Current incidents such as the collapse of the Carola Bridge in Dresden, Germany draw international attention to the importance of infrastructure monitoring.

In order to gain more knowledge on the structural response due to increasing loads and damages, laboratory load tests on a bridge girder were carried out. The bridge girder stems from a bridge partly collapsed due to flooding in summer 2024. More detailed information about the tested bridge beam and the test procedure can be derived from [1]. The aim of the controlled load tests was to determine the structural behavior and perform measurements at all damage states in order to get a better understanding for condition assessment. This can be done using different measurement techniques, which can be broadly categorized in point-wise and distributed sensors. Suitable point-wise sensors are e.g. accelerometers, but also static or dynamic Robotic Total Station (RTS) measurements [2][3] can deliver valuable results. The drawback of these point-wise techniques is that they require several sensors in order to monitor the structure, and all of them need to be mounted in appropriate positions to obtain meaningful results. Distributed Fiber Optic Sensing (DFOS) functions as a distributed sensor, where one fiber can precisely sense information along its entire

length. Different DFOS techniques can provide insights on the frequency behavior of the structure, but also on the bending due to the applied force. Furthermore, cracks appearing in the structure can be detected. The fiber can be glued on the structure, but also embedded directly inside the structure if it is newly constructed. The application of DFOS for bridge monitoring is currently becoming of more interest [4].

All of the mentioned measurement techniques were applied at the conducted laboratory tests. However, this paper focuses on the results and comparison of Distributed Acoustic Sensing (DAS) and accelerometers.

2 BRIDGE MONITORING WITH DFOS

The general principle of DFOS is light coupled into a glass fiber, which gets scattered at natural impurities at every point inside the fiber. A part of the light gets backscattered to the interrogation unit, where different information, especially temperature (T), strain (ϵ) or strain rates (ϵ/t), can be derived depending on the measured backscatter effect (see Figure 1). As the light propagates through the fiber, information is sensed along the entire length of the fiber, which can amount up to several tens of kilometers. Significant advantages of DFOS are immunity to electromagnetic interferences and only the small and lightweight fiber being needed on-site, a passive element which requires no power supply.

Since this paper focuses on Distributed Acoustic Sensing (DAS) only, the following paragraph will describe the working principle in more detail.

Pulsed light is coupled into the fiber with high frequency, whereby the maximum sampling frequency f_{max} is dependent on the fiber length L by

$$f_{max} = \frac{c}{2nL} \quad (1)$$

in order to avoid overlapping pulses in the fiber.

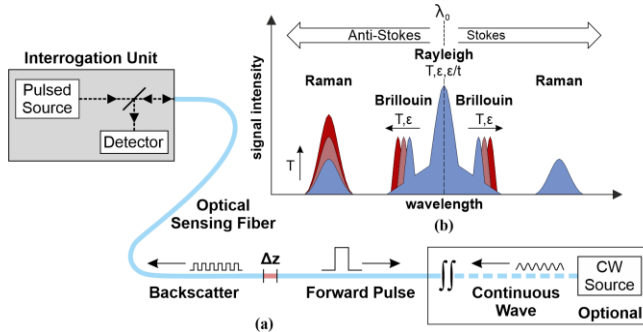


Figure 1. (a) Schematic representation of the operating principle of distributed fiber optic sensing techniques and (b) different backscatter effects, based on [5].

DAS interrogation units only detect and measure Rayleigh backscatter, which has the highest intensity [6]. Rayleigh backscatter is affected by strain and temperature changes, which in turn cause differences in the optical path length. The optical path length is determined from the differential phase between two scatter points [7]. Since the measurand is the optical phase change within a certain distance (the gauge length), the output consists of relative measurements describing the behavior of strain within a certain period of time, resulting in strain rate measurements. The gauge length is typically on the order of several meters and defines the spatial resolution of the measurement. Compared to other DFOS techniques, DAS provides lower spatial resolution, but much higher temporal resolution reaching up to several kHz, making it suitable for dynamic measurements.

The seamless high frequency measurements can provide valuable information about the structural integrity of a bridge by deploying only one fiber to the structure. By numerically integrating the derived strain rate measurements to strain, additional information about the strain distribution along the structure can be gained.

3 LOAD TESTS

3.1 Setup

The structure under test is a prestressed girder with a deck plate and has a length of about 10 m. It was placed in the laboratory of the Slovenian National Building and Civil Engineering Institute (ZAG) underneath a hydraulic actuator able to apply vertical load. More information about the placement of the girder on the testing facility can be found in [1]. Several sensors were mounted on the structure. The location of the sensors discussed in this paper can be seen in Figure 2, but also other sensors such as tilt sensors, RTS and camera have been used.

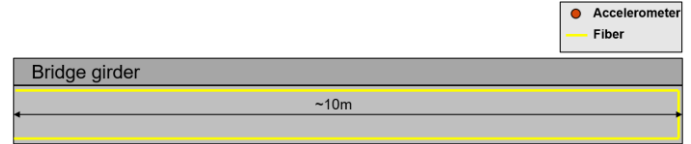


Figure 2. Schematic representation of tested structure with mounted sensors.

As also shown in Figure 3, the fiber was mounted on the upper and lower part of the girder along its entire length. A second fiber was glued in order to be able to perform simultaneous measurements with different DFOS techniques, which are not subject of this present paper. For the DAS measurements, the inner fiber was used.

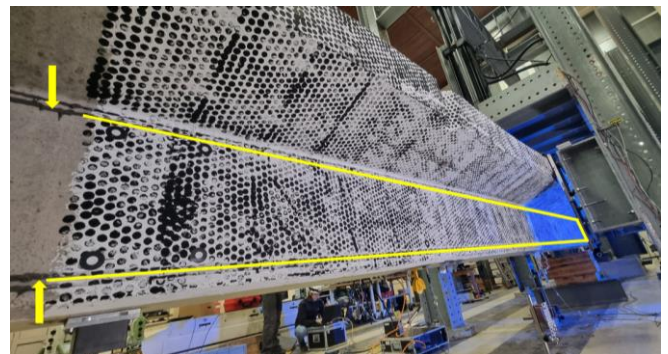


Figure 3. Glued fibers on the bridge girder placed in the laboratory.

The measurement settings for DAS and accelerometers were as stated in Table 1.

Table 1. Measurement settings.

	DAS	Accelerometers
Sampling frequency	5000 Hz	200 Hz
Measurement channels	25	3
Measurand	$\mu\text{m}/\text{m}/\text{s}$	m/s^2

3.2 Test procedure

The test procedure consisted of 10 load phases with 2 cycles each, increasing the maximum load with every phase. For the first three phases, the applied load was increased stepwise with a waiting time of 2 minutes after every load increment, while for the latter phases a constant linear load increase was applied. The loading speed was 1 kN/s, and the same procedure was applied for both loading and unloading. The load cycles are shown in Figure 4. Note that the pause between the load phases 3 and 4 is not shown correctly in the plot, since there was an overnight pause in between.

In between the phases, ambient vibration tests were performed. These aimed to stimulate the girder in a way so the eigenfrequencies could be detected. The stimulation was performed by a human jumping on the girder in order to induce an impulse. After phase 5, shaker tests were performed by placing a vertical shaker on the beam, stimulating it with different singular frequencies as well as with a frequency sweep.

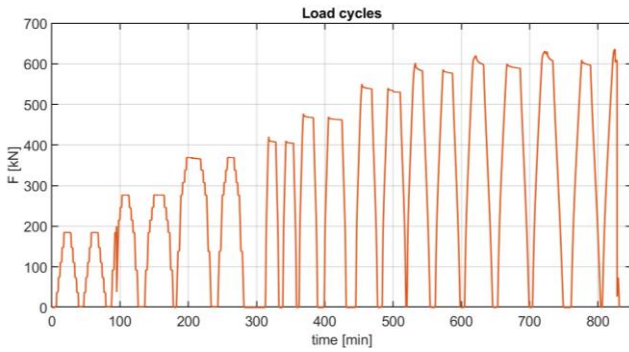


Figure 4. Performed load cycles.

3.3 Eigenfrequencies

The eigenfrequencies can be determined from the ambient vibration tests and provide significant information about the structural integrity, since a change in the eigenfrequency indicates structural damage. Figure 5 shows the ambient vertical vibration of the girder after phase 2, measured with the accelerometers at 3 discrete positions on the beam bottom.

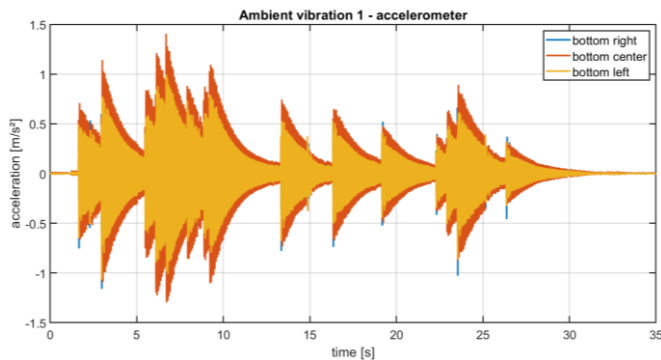


Figure 5. Accelerometer measurements of ambient vibration, 3 positions on the bottom.

DAS measurements can be obtained along the entire fiber. The occurring strain rates caused by the excitation of the girder can be seen in Figure 6, whereby the y-axis shows the distance along the fiber, and the x-axis depicts the change over time.

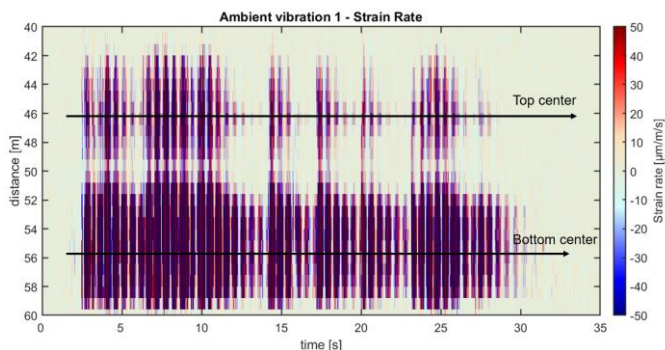


Figure 6. DAS waterfall plot of ambient vibration.

From the DAS waterfall plot, a location on the fiber close to the accelerometer can be selected. For comparison, a location at the bottom center and also in the upper center was chosen. Note

that the spatial resolution of the DAS amounts to 0.8 m. When compared with the accelerometers, it is noticeable that the measurements look very comparable with the single impacts being clearly differentiable in both (Figure 7). For better comparison, the DAS measurements have been down sampled to the same sampling frequency as the accelerometers (200 Hz). What stands out in the DAS measurement is the significant difference between the upper and lower part of the beam, with the lower section showing considerably more movement than the upper section. This indicates a high vertical position of the neutral axis. As the measured vibrations on the upper and lower fiber are in phase (see Figure 8.), the neutral axis must be located above the upper fiber.

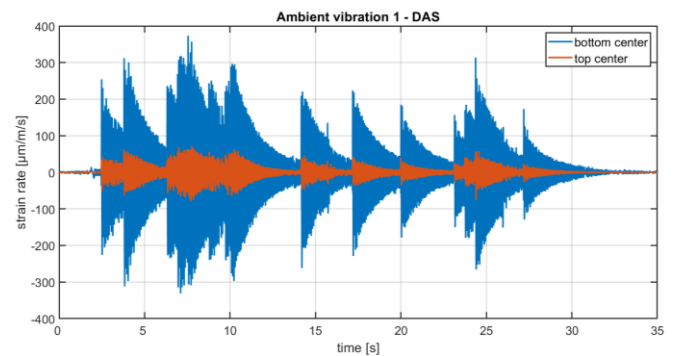


Figure 7. DAS measurements of ambient vibration, top and bottom center.

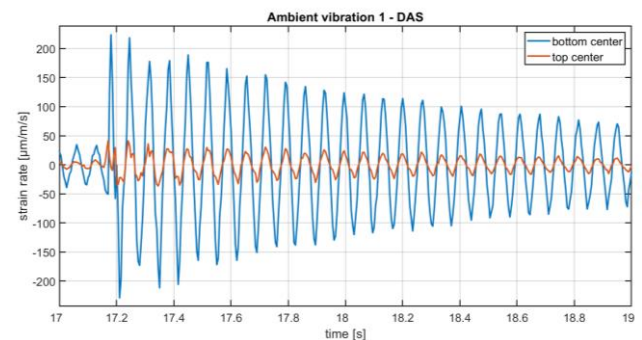


Figure 8. Measurements of upper and lower fiber are in phase for measurement of ambient vibration.

In order to determine the eigenfrequencies appearing through the excitation, a Short Time Fourier Transform (STFT) with a window length of 4 s was computed both for the accelerometers and DAS measurements. For the accelerometer mounted at the bottom center of the girder, the resulting amplitudes of each window are shown in Figure 9. The appearing main frequency amounts to 14.75 Hz. The same procedure was applied to the DAS measurements. Again, a bottom center position on the fiber, as well as a top center position were chosen for comparison. For both positions, the same eigenfrequency of 14.75 Hz was observed (Figure 10), which is in agreement with the accelerometer measurements shown in Figure 9.

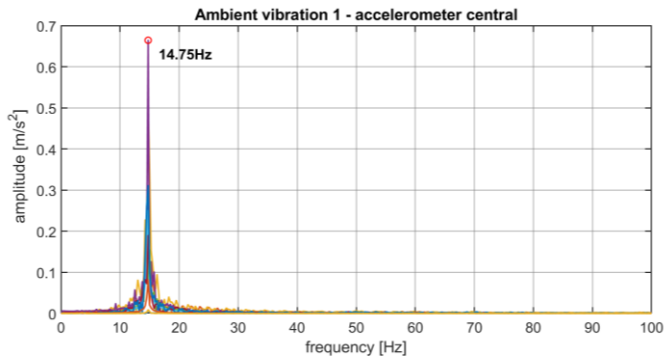


Figure 9. Eigenfrequency of the beam after loading phase 2, bottom center accelerometer.

However, the measured amplitudes at the bottom and top part vary significantly, with the bottom part responding about 5 times stronger than the top part (note the different scaling in Figure 10). This again implies a high vertical position of the zero line of the beam.

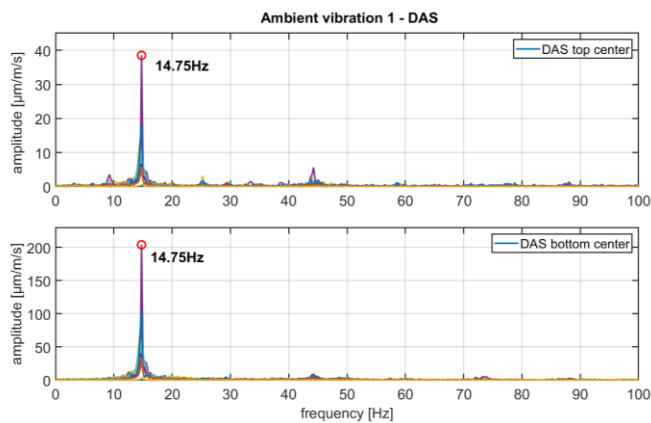


Figure 10. Eigenfrequency of the beam after loading phase 2, bottom and top center measured with DAS.

One of the main advantages of Distributed Fiber Optic Sensing is the seamless measurement along the entire fiber. The frequency and amplitude can be obtained at any point and give a more complete picture of the overall structural behavior. Therefore, a frequency analysis was carried out for every point along the fiber. The eigenfrequency of 14.75 Hz remained constant along the entire girder, but the amplitude varies strongly as it can be seen in Figure 11.

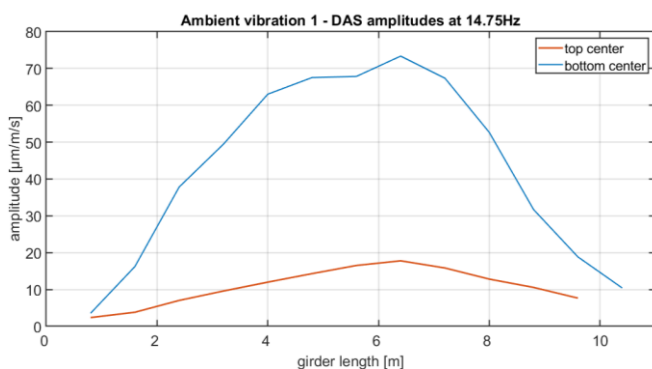


Figure 11. Amplitude curve for eigenfrequency of 14.75 Hz along the top and bottom part of the beam.

Note that the different dimension of the amplitudes compared to Figure 10 stems from the FFT being computed over the entire event, instead of 4 s windows. Again, it can be observed that the bottom part of the beam shows stronger reaction, and also the middle part of the beam shows increasing amplitudes for both the upper and lower side.

The eigenfrequencies have been determined for every ambient vibration event, which was carried out after each load phase. With increasing damage, the measured eigenfrequencies decrease significantly. The first cracks appeared in load phase 2. Table 2 shows the results for both DAS and accelerometers, which are in complete agreement for every measurement. Note that due to the window size of 4 s, the frequency resolution only amounts 0.25 Hz.

Table 2. Comparison of eigenfrequencies for DAS and accelerometers, ambient vibration at different damage states.

Impulse Excitation	After load phase	$f_{Acc.}$ [Hz]	f_{DAS} [Hz]
1	Phase 2	14.75	14.75
2	Phase 3	14.25	14.25
3	Phase 4	14.25	14.25
4	Phase 6	13.75	13.75
5	Phase 7	12.50	12.50
6	Phase 8	10.50	10.50
7	Phase 9	10.00	10.00

3.4 Shaker Tests

In addition to the ambient vibration tests, experiments with a shaker were carried out. The shaker weighs approx. 100 kg and can oscillate vertically. Different singular frequencies and amplitudes can be set, and also frequency or amplitude sweeps can be performed. The shaker was placed as close to the middle of the girder as possible (Figure 12).



Figure 12. Placement of the vertical shaker on the girder.

First, a frequency sweep from 2-100 Hz was carried out. After that, the shaker was operated with different constant frequencies but increasing amplitude. An overview of the test procedure is shown in Figure 13. The different amplitude sweeps can be clearly seen in the DAS raw data. A STFT shows in more detail the appearing frequencies and amplitudes. The frequency sweep ($t=100-350$ s) is visible well, with higher amplitudes appearing when the shaker frequency matches the eigenfrequency. Also, the second harmonics can be detected.

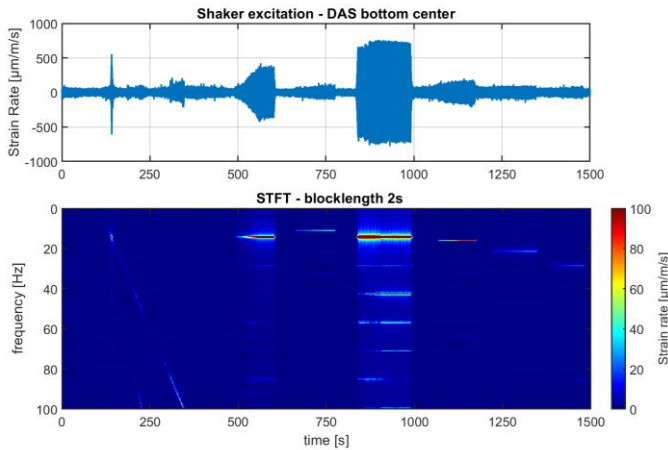


Figure 13. Overview shaker tests - raw data and STFT.

After that, the STFT with a window size of 2 seconds clearly shows the amplitude sweeps ($t=500-1500$ s) at different constant frequencies. A strong structural response can be detected when the input frequency amounts to the eigenfrequency or the latter is a harmonic of the stimulating frequency. This can be seen in the first ($t=500-600$ s) and third ($t=840-1000$ s) sweep, where the input frequency is 7.1 Hz and 14.2 Hz. Furthermore, a detailed look is taken at the excitation close to the eigenfrequency. Note that the eigenfrequency already decreased to 14.25 Hz, since the shaker tests were carried out after phase 5 (compare Table 2).

Taking a closer look at sweep 3, where the girder was stimulated with the eigenfrequency, also the harmonics can clearly be detected. This can be seen at the bottom position as well as at the upper position (Figure 14). The most dominant is the third harmonic at 42.6 Hz.

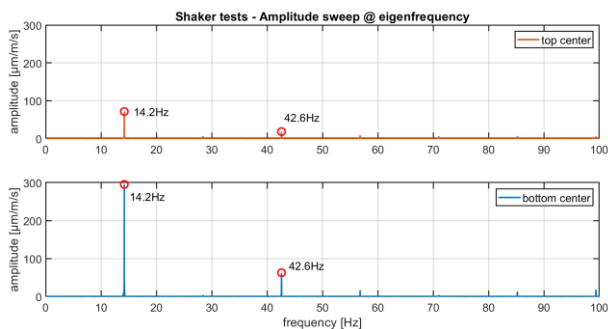


Figure 14. FFT at top and bottom center position.

3.5 Load Capacity

In addition to a frequency analysis, DFOS measurements can also serve to determine the applied strain on the structure. Typically, static DFOS measurements such as Optical Frequency Domain Reflectometry (OFDR) or Brillouin backscattering are used to measure absolute strain. These systems usually provide a better spatial resolution, but a poor sampling rate, if at all capable of performing dynamic measurements.

By numerically integrating the measured strain rates over time, the appearing strain can be calculated from the DAS

measurements. For this purpose, a known starting value (initial strain) is needed. In case of the load tests, this was accomplished by starting the measurement before any load is applied, thereby minimizing the induced integration error. However, this is based on the assumption that the fiber does not experience any permanent strain from the previous load cycles. Figure 15 shows a waterfall plot of the appearing strain along the entire fiber. The load increments can be seen as progressively increasing elongation of the fiber over time, as well as a clear difference between the upper and lower part of the beam.

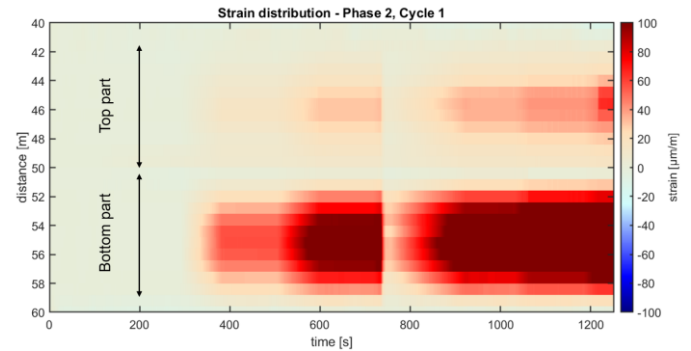


Figure 15. Waterfall plot of induced strain along the fiber, load phase 2.

Taking a closer look at the top and bottom center position of the girder, the load increments and pause time in between are visible (Figure 16), as well as the significant difference in strain between the upper and lower part. Note that the outlier in the load strain profile ($t=750-900$ s) derives from a failure of the hydraulic actuator.

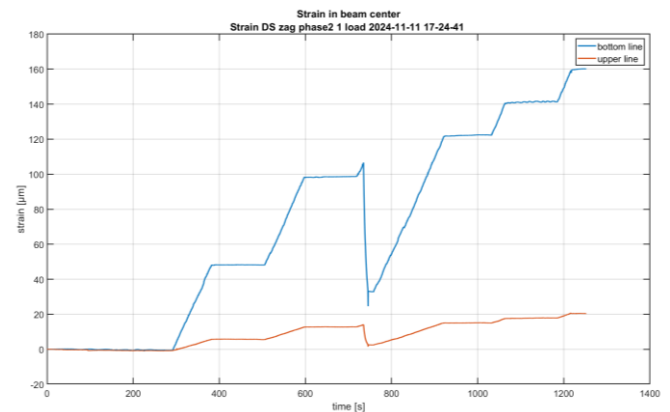


Figure 16. Increasing strain at top and bottom center, phase 2.

Figure 17 shows the strain distribution along the fiber for load phase 4, cycle 2. At this phase, there was no load incrementation followed by a waiting period, but a linear increase of the load until the maximum load. The applied load is approximately one third higher than in phase 2 (see Figure 4), which results in significantly higher strain. Figure 17 shows the loading as well as the unloading of the element.

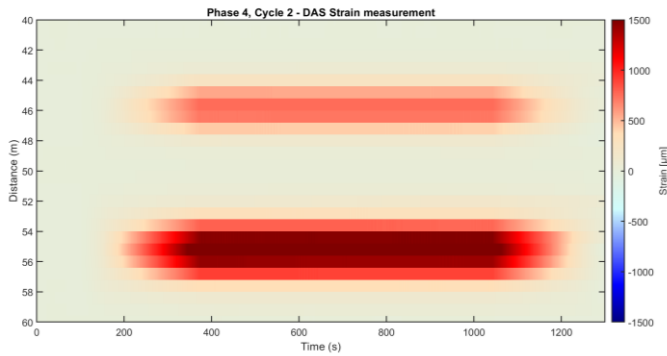


Figure 17. Waterfall plot of strain distribution, phase 4, cycle 2.

Of particular interest is the strain distribution, which appears very concentrated in the center of the girder, where the force is applied (Figure 18, right).

Also, a more detailed look can be taken at the strain distribution on the bottom and top center of the girder (Figure 18, left). The lower part experiences significantly higher strain, amounting more than twice as much as the upper part. It should also be noted that with increasing force the ratio of the measured strain between the lower and upper part increases, which implies an upwards moving neutral axis with increasing load.

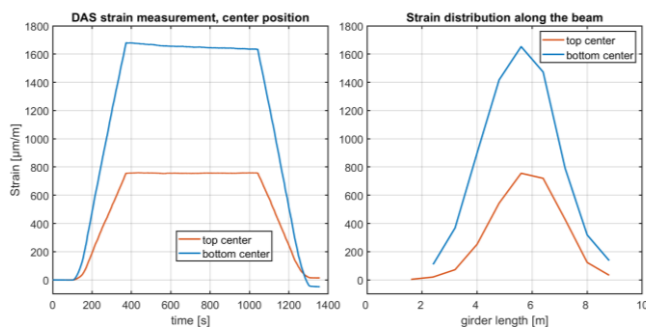


Figure 18. Load phase 4. Left: Measured strain at top and bottom center. Right: Strain distribution along the fiber at maximum load.

4 SUMMARY AND CONCLUSION

The loading tests have shown that Distributed Fiber Optic Sensing is a suitable measurement technique to determine the structural integrity of girders or bridges. While delivering comparable results to other sensing techniques, it can provide significant advantages compared to pointwise sensors. A frequency analysis can be performed seamlessly along the entire fiber, whereby the high sampling rates can determine any changes in the eigenfrequencies. In addition to the high frequency strain rate measurements, the occurring strain at the structure can also be determined. The obtained results can provide valuable insights about the damage state of the structure. All this information can be sensed with only one fiber mounted to the structure, whereby after the initial installation no further direct interaction with the structure is necessary.

Further work will include a deeper look on detecting the tearing of tension cables, as well as a more detailed look on damage assessment using mode shapes.

ACKNOWLEDGMENTS

We want to acknowledge the collaboration with the Slovenian National Building and Civil Engineering Institute (ZAG), which carried out the load tests at their laboratory and gave us the opportunity to install our sensors and carry out the measurements.

REFERENCES

- [1] M. Kreslin, M. Kosič, A. Šajna, A. Anžlin, D. Hekič, V. Požonec and P. Triller, Laboratory Testing of Old Bridge Girders: Preliminary Results, *SHMII-13 Proceedings*, Graz, Austria, September 2025.
- [2] P. Psimoulis and C. Stiros, Measuring Deflections of a Short-Span Railway Bridge Using a Robotic Total Station, *Journal of Bridge Engineering*, 18(2): 182-18, 2013.
- [3] C. Schönberger, W. Lienhart and T. Moser, Dynamic monitoring of civil infrastructures with geodetic sensors, in *Proceedings 5th Joint International Symposium on Deformation Monitoring JISDM*, pp. 537-543, 2022.
- [4] M. Morgese, C. Wang, T. Taylor and F. Ansari, Distributed Operational Modal Analysis of Multispan Bridges, *Journal of Bridge Engineering*, 30(5), 2025.
- [5] C. Monsberger and W. Lienhart, Distributed Fiber Optic Shape Sensing of Concrete Structures, *Sensors* 2021, 21, 6098, 2021.
- [6] A. H. Hartog, *An Introduction to Distributed Optical Fibre Sensors*. CRC Press, Taylor & Francis Group, 2017.
- [7] Febus Optics SAS, Technical User Guide Febus A1-R, Version 9, Pau, France, 2023.